Simultaneous Localization and Communication Methods

Using Short-Time and Narrow-Band Acoustic Signals

Masanari Nakamura

Hokkaido University
Sapporo 060-0814, Japan
Email: masanari@ist.
hokudai.ac.jp

Hiromichi Hashizume

National Institute of Informatics
Tokyo 101-8430, Japan
Email: has@nii.ac.jp

Masanori Sugimoto

Hokkaido University
Sapporo 060-0814, Japan
Email: sugi@ist.
hokudai.ac.jp

Abstract—In this paper, we describe simultaneous localization and communication methods using acoustic signals transmitted simultaneously from multiple speakers. In the case where short-time and narrow-band acoustic signals are used, the interference of signals could cause a systematic error of localization and communication depending on the modulation value. To reduce this systematic error, a noninterference region was constituted in the received signal, and localization and demodulation were processed using this region. Through simulation and real-environment experiments, it was confirmed that the proposed method can reduce the systematic error.

Keywords–indoor localization; TDoA; acoustic signal; acoustic communication; DPSK.

I. INTRODUCTION

Mobile devices, such as smartphones, tablets, and smart glasses are widely used nowadays. Complementing these is the location data of mobile devices, which are employed in various services. Outside a building, mobile devices can precisely locate themselves via the Global Navigation Satellite System (GNSS). However, inside a building, the GNSS could make large errors due to shielding. To circumvent this, alternative methods for indoor environments have been widely researched [1].

In this paper, we describe the indoor localization method using acoustic signals. Acoustic signals simultaneously transmitted by speakers installed in an indoor environment are captured by a microphone. The location of the microphone is estimated by using the Time Difference of Arrival (TDoA) of these signals. As a microphone is embedded in mobile devices, this system can localize mobile devices without any additional hardware.

With regard to localization performance, the precision of localization mainly depends on the transmitted signal. In general, the wider the bandwidth of the signal, the more precise is the TDoA estimation. However, from the viewpoint of scalability, it is desirable to have as narrow a bandwidth as possible. Similarly, the longer the length of the signal, the more precise is the TDoA estimation due to the signal-to-noise ratio (SNR). However, from the viewpoint of the update rate, it is desirable that the length of the signal be as short as possible.

Herein, if signals for localization can contain some information, it simultaneously enables acoustic communication. Therefore, acoustic signals can be used more efficiently and could expand the range of applications. For indoor acoustic communication, some methods have been proposed [2][3]. As errors due to multipath propagation occur, using Differential Phase-Shift Keying (DPSK) is desirable as it can cancel these errors. However, if short-time and narrow-band acoustic signals are used, the communication performance deteriorates due to interference between the signals transmitted simultaneously by different speakers. In addition, when the acoustic signals are modulated, the estimated TDoA have systematic errors depending on the modulated values.

In this paper, we propose simultaneous localization and communication methods that can reduce the above systematic error using short-time and narrow-band signals. In the received signal of our proposed method, there is a region where each signal is orthogonal to each other. As the TDoA estimation and demodulation are processed using this region, our proposed method reduces the systematic error due to interference.

To concisely discuss the influence of signal interference on localization and communication, we evaluated the azimuth estimation performance by the TDoA of two speakers as one-dimensional localization.

The remainder of this paper is structured as follows. Section II shows the details of the issues dealt with herein and the related research. Section III describes the proposed method. In Section IV, comparative evaluations of the conventional and proposed methods, performed under simulation and real environments are discussed. Section V presents the experimental results and discussions. Conclusions are provided in Section VI.

II. RELATED WORK

Herein, we describe the problem while performing azimuth estimation using two speakers and communication by DPSK simultaneously using short-time and narrow-band signals. To describe these processes of transmitting and receiving acoustic signals, we use the chirp signals as an example. The i-th signals simultaneously transmitted from the left and right speakers are

$$s_R^i(t) = \begin{cases} \sin(2\pi(f_1 t + \frac{1}{2}\alpha_{12}t^2) + \phi_i^R) & 0 \le t \le T \\ 0 & otherwise \end{cases} \quad (1)$$

$$s_L^i(t) = \begin{cases} \sin(2\pi(f_3 t + \frac{1}{2}\alpha_{34}t^2) + \phi_i^L) & 0 \le t \le T \\ 0 & otherwise \end{cases} \quad (2)$$
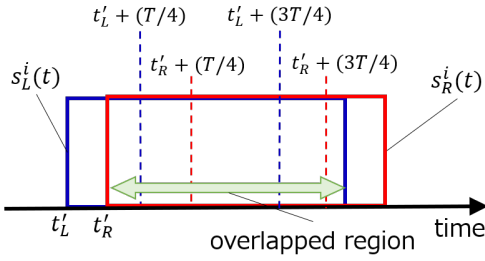
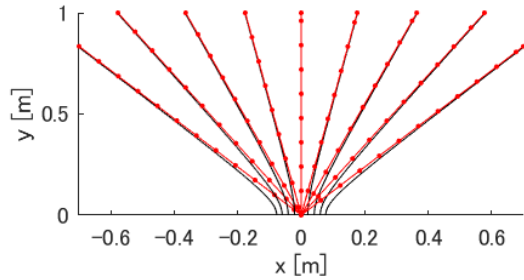Figure 1. Illustration of the received signals.

Figure 2. Hyperbola of TDoA (black lines) and its asymptote (red lines).

where ϕ_i^R and ϕ_i^L are DPSK modulation values and $\alpha_{12} = (f_2 - f_1)/T$, $\alpha_{34} = (f_4 - f_3)/T$. We call these signals a symbol. The received signal can be expressed as

$$r^i(t) = a_R s_R^i(t - t_R) + a_L s_L^i(t - t_L) \qquad (3)$$

where t_R and t_L represent the reception times of the left and right signals of the speaker. The analytic signals corresponding to the above signals are

$$e_R(t) = \begin{cases} \exp(j2\pi(f_1 t + \frac{1}{2}\alpha_{12}t^2)) & 0 \leq t \leq T \\ 0 & otherwise \end{cases} \qquad (4)$$

$$e_L(t) = \begin{cases} \exp(j2\pi(f_3 t + \frac{1}{2}\alpha_{34}t^2)) & 0 \leq t \leq T \\ 0 & otherwise \end{cases} \qquad (5)$$

The received signal is processed using the matched filter with analytic signals as follows:

$$\begin{aligned} c_R^i(t) &= \int_t^{t+T} r^i(\tau)e_R(\tau - t)d\tau \\ &= \int_t^{t+T} a_R s_R^i(\tau - t_R)e_R(\tau - t)d\tau \\ &+ \int_t^{t+T} a_L s_L^i(\tau - t_L)e_R(\tau - t)d\tau \end{aligned} \qquad (6)$$

The reception time of speaker R is estimated as follows:

$$t_R = \arg \max_t |c_R^i(t)| \qquad (7)$$

If the second term $\int_t^{t+T} s_L^i(\tau - t_L)e_R(\tau - t)d\tau$ in (6) is not zero, the time that has the maximum value of $|c_R^i(t)|$ could not match the true reception time, and some error occurs in the estimated value of the reception time. As the phases of each term in (6) depend on ϕ_i^R and ϕ_i^L in (1) and (2), the error in reception time could change depending on the DPSK modulation value. To calculate TDoA, a similar process is

applied to estimate the reception time of speaker L's signal t_L; subsequently, an error of the same type occurs in t_L estimation.

When the following the Orthogonal Frequency Division Multiplexing (OFDM) signals are used instead of chirp signals, the above systematic error would occur. This is because $s_R^i(t)$ and $s_L^i(t)$ are not orthogonal except where the microphone is located at the same distance from the speakers R and L.

$$s_R^i(t) = \begin{cases} \sum_{k=1}^{K} \sin(2\pi f_k^R t + \psi_k^R + \phi_i^R) & 0 \leq t \leq T \\ 0 & otherwise \end{cases} \qquad (8)$$

$$s_L^i(t) = \begin{cases} \sum_{k=1}^{K} \sin(2\pi f_k^L t + \psi_k^L + \phi_i^L) & 0 \leq t \leq T \\ 0 & otherwise \end{cases} \qquad (9)$$

In (8), (9), ψ_K^R and ψ_k^L are the initial phases that determine the waveform of the OFDM signal.

The second term in (6) that represents interference decreases as the length and bandwidth of the signal increase. Therefore, in conventional methods, such as chirp signal-based [4][5], OFDM-based [6][7][8], and CDMA-based methods [9][10][11][12], and random signal methods [13][14], interference was avoided by setting the length and bandwidth of signals to sufficiently large values.

In this paper, we propose a method that can reduce the above systematic errors with short-time and narrow-band signals. Our proposed method is an extension of the localization method FDM-PAM [15][16][17] to enable simultaneous communication.

III. PROPOSED METHOD

In this section, we propose simultaneous localization and communication methods that can reduce the systematic error using short-time and narrow-band signals.

A. Transmission Signal

In our proposed method, the speakers R and L transmit the following signals simultaneously,

$$s_R^i(t) = \\ \begin{cases} \sin(2\pi f_1 t + \phi_i^R) + \sin(2\pi f_2 t + \phi_i^R + \pi) & 0 \leq t \leq T \\ 0 & otherwise \end{cases} \qquad (10)$$

$$s_L^i(t) = \\ \begin{cases} \sin(2\pi f_3 t + \phi_i^L) + \sin(2\pi f_4 t + \phi_i^L + \pi) & 0 \leq t \leq T \\ 0 & otherwise \end{cases} \qquad (11)$$

where frequency f_n is set to $f_n = f_1 + ((n-1)/(T/2))$.

B. TDoA Estimation and Demodulation

The process of TDoA estimation for the i-th symbol is described below. The signals transmitted from the left and right speakers are received by the microphone as follows:

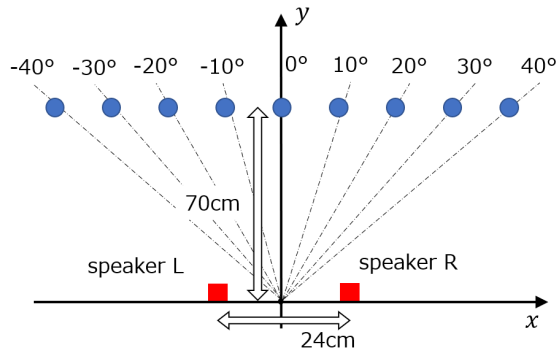$$r^i(t) = a_R s_R^i(t - t_R) + a_L s_L^i(t - t_L) \qquad (12)$$
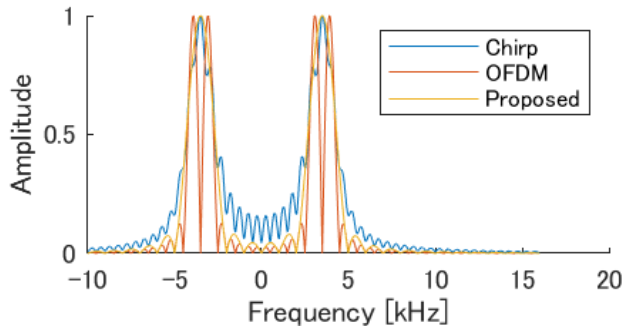
Figure 3. Speaker and microphone arrangement.

Figure 4. Frequency spectrum of the signal transmitted by speaker R.

The received signal is processed using the matched filter with analytic signals as follows:

$$e_R(t) = \begin{cases} \exp(j2\pi f_1 t) + \exp(j(2\pi f_2 t + \pi)) & 0 \leq t \leq T \\ 0 & otherwise \end{cases} \quad (13)$$

$$e_L(t) = \begin{cases} \exp(j2\pi f_3 t) + \exp(j(2\pi f_4 t + \pi)) & 0 \leq t \leq T \\ 0 & otherwise \end{cases} \quad (14)$$

Calculate the temporary reception time t'_R, t'_L as follows.

$$t'_R = \arg\max_t |c^i_R(t)| \quad (15)$$

$$t'_L = \arg\max_t |c^i_L(t)| \quad (16)$$

where c^i_R and c^i_L are

$$c^i_R(t) = \int_t^{t+T} r^i(\tau) e_R(\tau - t) d\tau \quad (17)$$

$$c^i_L(t) = \int_t^{t+T} r^i(\tau) e_L(\tau - t) d\tau. \quad (18)$$

Figure 1 indicates an illustration of received signal. Here, suppose the absolute value of TDoA $|\Delta t| = |t_L - t_R|$ is less than $T/4$. From the definition of f_n and the appendix, if the signal of length $T/2$ is cut out of the overlapped region of the received signal (Figure 1), sine waves that compose the cut-out signal are mutually orthogonal. As shown in Figure 1, the signal of length $T/2$ is obtained by cutting out a region from $t'_L + (T/4)$ to $t'_L + (3T/4)$ or from $t'_R + (T/4)$ to $t'_R + (3T/4)$.

In the following, t_{max} is the reference time of cutting out. To avoid the error due to the influence of (17), (18), t_{max} is set to t'_R or t'_L as follows. $|c^i_R(t'_R)|$ is larger than or equal to $|c^i_L(t'_L)|$, t_{max} is set to t'_R. If $|c^i_R(t'_R)|$ is less than $|c^i_L(t'_L)|$, t_{max} is set to t'_L. In this section, we take $t_{max} = t'_R$ as an example. The same is obviously true for the case of $t'_{max} = t_L$.

The cut-out signal $r^i_c(t)$ is represented as follows:

$$\begin{aligned} r^i_c(t) = &\, a_R \sin(2\pi f_1(t + t_{max} + \frac{T}{4}) + \phi^R_i) \\ &+ a_R \sin(2\pi f_2(t + t_{max} + \frac{T}{4}) + \phi^R_i) \\ &+ a_L \sin(2\pi f_3(t + t_{max} + \frac{T}{4} + \Delta t) + \phi^L_i) \\ &+ a_L \sin(2\pi f_4(t + t_{max} + \frac{T}{4} + \Delta t) + \phi^L_i) \end{aligned} \quad (19)$$

where $r^i_c(t) = 0$ for $t < 0, t > T/2$. To obtain the phase value of each sine wave of (19), the inner product of $r^i_c(t)$ and complex sine wave is calculated as follows:

$$c^i_n = \int_0^{T/2} r^i_c(t) \exp(-j2\pi f_n t) dt \quad (20)$$

c^i_1, c^i_2, c^i_3 and c^i_4 can be represented as follows (see Appendix for details):

$$c^i_1 = \frac{a_R T}{4j} \exp(j(2\pi f_1(t_{max} + \frac{T}{4}) + \phi^R_i)) \quad (21)$$

$$c^i_2 = \frac{a_R T}{4j} \exp(j(2\pi f_2(t_{max} + \frac{T}{4}) + \phi^R_i)) \quad (22)$$

$$c^i_3 = \frac{a_L T}{4j} \exp(j(2\pi f_3(t_{max} + \frac{T}{4} + \Delta t) + \phi^L_i)) \quad (23)$$

$$c^i_4 = \frac{a_L T}{4j} \exp(j(2\pi f_4(t_{max} + \frac{T}{4} + \Delta t) + \phi^L_i)). \quad (24)$$

The phase values of $jc^i_1, jc^i_2, jc^i_3, jc^i_4$ can be calculated as follows:

$$\phi^i_1 = 2\pi f_1(t_{max} + \frac{T}{4}) + \phi^R_i \quad (25)$$

$$\phi^i_2 = 2\pi f_2(t_{max} + \frac{T}{4}) + \phi^R_i \quad (26)$$

$$\phi^i_3 = 2\pi f_3(t_{max} + \frac{T}{4} + \Delta t) + \phi^L_i \quad (27)$$

$$\phi^i_4 = 2\pi f_4(t_{max} + \frac{T}{4} + \Delta t) + \phi^L_i \quad (28)$$

The phase differences of each speaker's signal are

$$\begin{aligned} \phi^i_2 - \phi^i_1 &= 2\pi(f_2 - f_1)(t_{max} + \frac{T}{4}) + (\phi^R_i - \phi^R_i) \\ &= 2\pi \frac{1}{T/2}(t_{max} + \frac{T}{4}) \end{aligned} \quad (29)$$

$$\begin{aligned} \phi^i_4 - \phi^i_3 &= 2\pi(f_4 - f_3)(t_{max} + \frac{T}{4} + \Delta t) + (\phi^L_i - \phi^L_i) \\ &= 2\pi \frac{1}{T/2}(t_{max} + \frac{T}{4} + \Delta t). \end{aligned} \quad (30)$$

from the definition of f_n. Therefore, TDoA Δt can be calculated as follows:

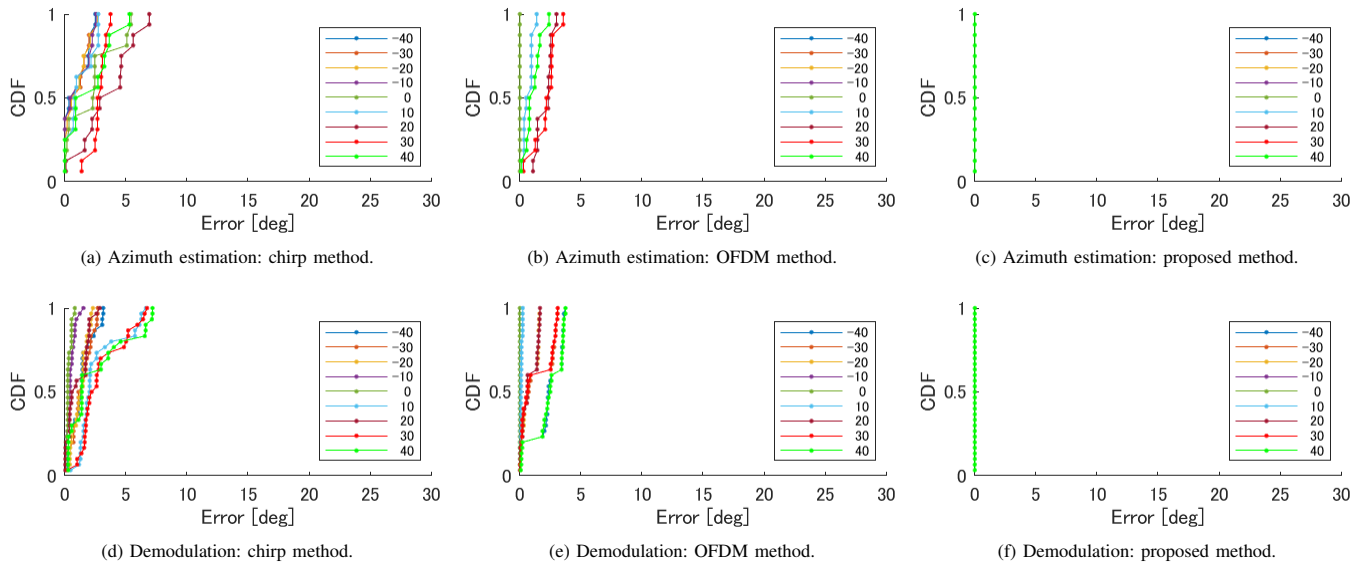$$\Delta t = \frac{(\phi^i_4 - \phi^i_3) - (\phi^i_2 - \phi^i_1)}{2\pi}(T/2) \quad (31)$$

(a) Azimuth estimation: chirp method.

(b) Azimuth estimation: OFDM method.

(c) Azimuth estimation: proposed method.

(d) Demodulation: chirp method.

(e) Demodulation: OFDM method.

(f) Demodulation: proposed method.

Figure 5. Simulation results (Legends indicate the azimuth θ of the microphone's location).

TABLE I. ENCODED VALUES.

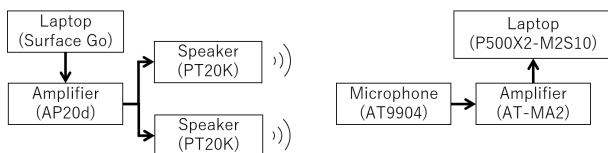| i	1	2	3	4	5	6	7	8	9	10	11	12	13	14	15	16
Φ_i^R	0	$\frac{\pi}{4}$	$\frac{\pi}{2}$	$\frac{3\pi}{4}$	0	$\frac{\pi}{4}$	$\frac{\pi}{2}$	$\frac{3\pi}{4}$	0	$\frac{\pi}{4}$	$\frac{\pi}{2}$	$\frac{3\pi}{4}$	0	$\frac{\pi}{4}$	$\frac{\pi}{2}$	$\frac{3\pi}{4}$
Φ_i^L	0	$\frac{\pi}{4}$	$\frac{\pi}{2}$	$\frac{3\pi}{4}$	$\frac{\pi}{4}$	$\frac{\pi}{2}$	$\frac{3\pi}{4}$	0	$\frac{\pi}{2}$	$\frac{3\pi}{4}$	0	$\frac{\pi}{4}$	$\frac{3\pi}{4}$	0	$\frac{\pi}{4}$	$\frac{\pi}{2}$

Figure 6. Experimental setup for the real environment.

Figure 7. Experimental environment.

In (29) and (30), the modulation values ϕ_i^R and ϕ_i^L are canceled out. Therefore, our proposed method can obtain TDoA without systematic error due to modulation values.

In our proposed method, signals are demodulated by using phase difference between successive symbols [18]. As the reference time of demodulation, we utilized the first symbol's t_{max}.

C. Azimuth Estimation

In this section, we describe the process of converting TDoA Δt to azimuth. The relation between TDoA Δt and the locations of speakers and a microphone is as follows:

$$c\Delta t = \sqrt{(\boldsymbol{x}_L - \boldsymbol{x})^T(\boldsymbol{x}_L - \boldsymbol{x})} - \sqrt{(\boldsymbol{x}_R - \boldsymbol{x})^T(\boldsymbol{x}_R - \boldsymbol{x})} \tag{32}$$

where $\boldsymbol{x}_R$, $\boldsymbol{x}_L$, $\boldsymbol{x}$ denote the 2D locations of the speakers R, L, and the microphone. c denotes the speed of sound.

Equation (32) indicates a hyperbola. The hyperbola asymptotically approaches a straight line passing through the origin.
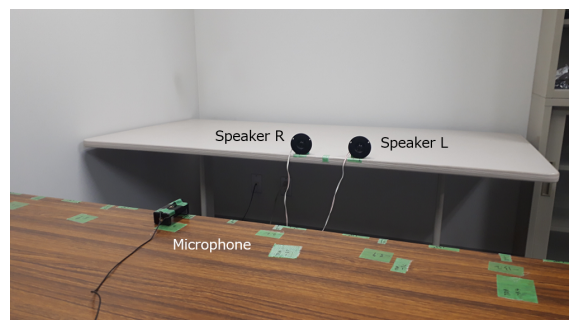
Hence, the azimuth can be calculated using this straight line. Figure 2 shows the hyperbola of TDoA and its asymptote. In Figure 2 the length of baseline is set to 24 cm. In this paper, the front direction of the speakers is set to 0 degree and the right direction is set to positive, as shown in Figure 3. The azimuth θ can be calculated by using TDoA Δt as follows:

$$\theta = \tan^{-1}\left(\frac{c\Delta t}{\sqrt{B^2 - c^2\Delta t^2}}\right) \tag{33}$$

where B is the length of the baseline.

IV. EXPERIMENTS

In this section, we conduct simulation and real-environment experiments.

A. Simulation Experiments

1) Experimental Setting: To evaluate the influence of interference and modulation, we conduct the following simulation experiment. Chirp signals and OFDM signals are used for comparison with our proposed method. The chirp signals are given by (1) and (2), and its parameters are $f_1 = 2.5$ kHz, $f_2 = 4.5$ kHz, $f_3 = 4.5$ kHz, $f_4 = 6.5$ kHz, and $T = 2$ ms. The OFDM signals are given by (8), (9), and its parameters
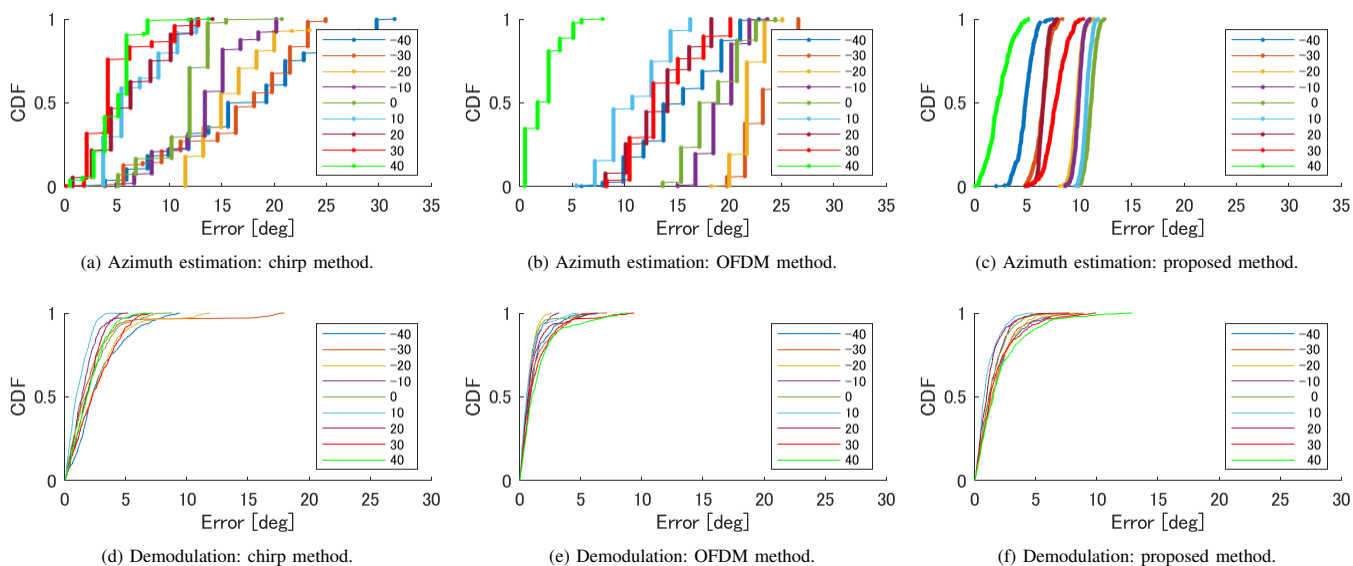
(a) Azimuth estimation: chirp method.

(b) Azimuth estimation: OFDM method.

(c) Azimuth estimation: proposed method.

(d) Demodulation: chirp method.

(e) Demodulation: OFDM method.

(f) Demodulation: proposed method.

Figure 8. Measurement results of the proposed method (Legends indicate the azimuth θ of the microphone's location).
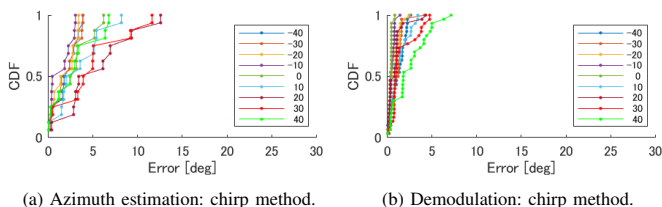

(a) Azimuth estimation: chirp method.

(b) Demodulation: chirp method.

Figure 9. Simulation results that reflect the amplitude of received signals.

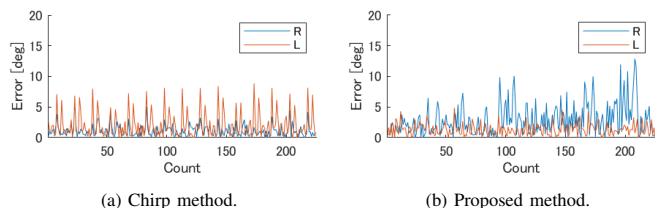(a) Chirp method.

(b) Proposed method.

Figure 10. Demodulation error of each symbol (Legends indicate speaker).

are $f_1 = 3$ kHz, $f_2 = 4$ kHz, $f_3 = 5$ kHz, $f_4 = 6$ kHz, $\psi_1^R = \psi_1^L = 0$, $\psi_2^R = \psi_2^L = \pi$ and $T = 2$ ms. To evaluate the validity of these method as a comparator, we compare the frequency spectrum of these method. In Figure 4, although the frequency spectrum of each method does not match, the bandwidths are almost the same. Thus, the chirp and OFDM signals are considered to be appropriate as a comparator. We call the localization with these signals as the chirp method and OFDM method, respectively. The reception times of these methods are estimated by the matched filter. The parameters of the proposed method are $f_1 = 3$ kHz, $f_2 = 4$ kHz, $f_3 = 5$ kHz, $f_4 = 6$ kHz, and $T = 2$ ms. To avoid the effects of aliasing, the sampling rate was set to 960 kHz. Figure 3 shows the location of the speakers and a microphone. The microphone's locations were 9 points, which correspond to the azimuths of -40 degrees

to 40 degrees in steps of 10 degrees shown in Figure 3. In this simulation, the amplitudes of the received signals were set to the same value for all locations. The number of symbol values of ϕ_i^R and ϕ_i^L was set to 4. To cover all combinations of ϕ_i^R and ϕ_i^L, the values of symbol sequence were set as shown in Table I.

2) Results: Figure 5 shows the azimuth estimation error and demodulation error of DPSK for each location. Figures 5a and 5d show that a systematic error occurs in the chirp method due to interference between the signals transmitted by speakers R and L at all locations. Figures 5b and 5e show that a systematic error occurs in the OFDM method due to interference without the location where the azimuth θ equals 0 degree. This is because TDoA is zero at $\theta = 0$ degree. Figures 5c and 5f shows that our proposed method has no systematic error due to interference at all locations.

B. Real Environmental Experiments

1) Experimental Settings: To confirm the effectiveness of our proposed method, we conducted experiments in a real environment. The signals and locations of the speakers and a microphone are the same as in the simulation experiments. In the real-environment experiments, the symbol sequence having the encoded values in Table I were measured 15 times at each location. Therefore, the number of localizations was $15 \times 16 = 240$ and the number of demodulation values was $15 \times 15 = 225$. The transmission interval of symbols was set to 100 ms.

The configuration of the measurement system is shown in Figure 6. For the transmission system, we used a tablet PC (Microsoft Surface Go) as a signal generator, an amplifier (Fostex AP20d), and speakers (Fostex PT20K). For the receiving system, we used a microphone (Audiotechnica AT9904), an amplifier (Audiotechnica AT-MA2), and a laptop (Mouse Computer m-Book P500X2-M2S10) as the recorder. The sampling rate was set to 48 kHz. Figure 7 shows the experimental environment.

2) Results: Figure 8 shows the azimuth estimation and demodulation error of each location. With regard to azimuth estimation, our proposed method shows the best estimation performance from Figures 8a, 8b, and 8c. The standard deviation of azimuth estimation by the chirp, OFDM, and proposed methods were within 7.36, 3.93, and 1.15 degrees, respectively. As for DPSK, the demodulation performance of each method were similar in Figures 8d, 8e, and 8f. The standard deviation of demodulation by the chirp, OFDM, and proposed methods were within 3.73, 2.27, and, 2.95 degrees, respectively.

V. Discussion

In this section, we discuss the cause for systematic and random errors in real-environment experiments.

A. Systematic error of azimuth estimation

According to Figures 5 and 8, there are clear differences between simulation and real-environment experiments, and the received noises are not enough to explain these differences. In this section, we discuss the causes for this mismatch. In our proposed method, although systematic errors depending on the modulation value do not occur, there are some systematic errors at each location. We consider that these errors are caused by multipath signals reflected from the walls or ceilings in the room as there is no law on the relation between systematic errors and locations.

According to the conventional methods, in addition to the multipath signals, the amplitude of the received signal that depends on the location could be one of the reasons. Therefore, we conducted simulations that consider the received amplitude of real-environment experiments. Figure 9 shows the results of these simulations of the chirp method. These figures show that the systematic errors change in response to the received amplitude. Thus, in the conventional methods, the received amplitude is a factor in the difference of the systematic error between simulation and real-environment experiments.

B. Random error of demodulation

In this section, we discuss the reason why the standard deviation of the proposed method tends to be larger than the OFDM method, as shown in Section IV. Figure 10 shows the error of each symbol for the 16-symbol sequence (Table I) repeated 15 times at the received location with maximum standard deviation. Although the errors of the chirp method in Figure 10a contains periodic systematic errors and random errors, its random error is smaller than that of the proposed method (Figure 10b) as the signal length used in the OFDM method is twice as long as in our proposed method. Therefore, our proposed method has a disadvantage in terms of SNR, and its performance might be worse than conventional methods when systematic errors are small.

VI. Conclusions

In this paper, we proposed highly precise localization and communication methods using short-time and narrow-band acoustic signals. The simulation and real-environment experiments showed that our proposed method could reduce systematic errors compared to the conventional methods as interference between the acoustic signals could be avoided.

Appendix

The inner product of the sine wave and the complex sine wave can be defined as

$$\int_0^T \sin(2\pi f_a t + \phi)\exp(-j2\pi f_b t)dt$$
$$=\frac{T}{2j}\exp(j(\frac{(2\pi(f_a - f_b)T)}{2}))\text{sinc}(\frac{2\pi(f_a - f_b)T}{2})$$
$$-\frac{T}{2j}\exp(-j(\frac{2\pi(f_a + f_b)T}{2} + \phi))\text{sinc}(\frac{2\pi(f_a + f_b)T}{2})$$
(34)

where $\text{sinc}(x)$ is the sinc function $\text{sinc}(x) = \sin(x)/x$. If $2\pi(f_a + f_b)T/2$ is set to a large enough value,

$$\int_0^T \sin(2\pi f_a t + \phi)\exp(-j2\pi f_b t)dt$$
$$\approx \frac{T}{2j}\exp(j(\frac{2\pi(f_a - f_b)T}{2}))\text{sinc}(\frac{2\pi(f_a - f_b)T}{2}) \quad (35)$$

If $(f_a - f_b)T$ is an integer and non-zero value, Equation (35) is 0. This means that the sine wave $\sin(2\pi f_a t + \phi)$ and the complex sine wave $\exp(-j2\pi f_b t)$ are orthogonal.

References

[1] J. Xiao, Z. Zhou, Y. Yi, and L. M. Ni, "A survey on wireless indoor localization from the device perspective," ACM Comput. Surv., vol. 49, no. 2, 2016, pp. 1–31.

[2] H. Shen, S. Machineni, C. Gupta, and A. Papandreou-Suppappola, "Time-varying multichirp rate modulation for multiple access systems," IEEE Signal Processing Letters, vol. 11, no. 5, 2004, pp. 497–500.

[3] R. Dutta, A. B. J. Kokkeler, R. v. d. Zee, and M. J. Bentum, "Performance of chirped-fsk and chirped-psk in the presence of partial-band interference," in Proc. of SCVT, 2011, pp. 1–6.

[4] F. Höflinger et al., "Acoustic self-calibrating system for indoor smartphone tracking (assist)," in Proc. of IPIN, 2012, pp. 1–9.

[5] P. Lazik and A. Rowe, "Indoor pseudo-ranging of mobile devices using ultrasonic chirps," in Proc. of Sensys, 2012, pp. 99–112.

[6] M. O. Khyam, M. J. Alam, A. J. Lambert, M. A. Garratt, and M. R. Pickering, "High-precision ofdm-based multiple ultrasonic transducer positioning using a robust optimization approach," IEEE Sensors Journal, vol. 16, no. 13, 2016, pp. 5325–5336.

[7] M. O. Khyam, S. S. Ge, X. Li, and M. Pickering, "Orthogonal chirp-based ultrasonic positioning," Sensors, vol. 17, no. 5, 2017, pp. 1–14.

[8] M. O. Khyam, S. S. Ge, X. Li, and M. R. Pickering, "Pseudo-orthogonal chirp-based multiple ultrasonic transducer positioning," IEEE Sensors Journal, vol. 17, no. 12, 2017, pp. 3832–3843.

[9] F. J. Álvarez, T. Aguilera, and R. López-Valcarce, "Cdma-based acoustic local positioning system for portable devices with multipath cancellation," Digital Signal Processing, vol. 62, 2017, pp. 38–51.

[10] M. Hazas and A. Hopper, "Broadband ultrasonic location systems for improved indoor positioning," IEEE Trans. on Mobile Computing, vol. 5, no. 5, 2006, pp. 536–547.

[11] M. Alloulah and M. Hazas, "An efficient cdma core for indoor acoustic position sensing," in Proc. of IPIN, 2010, pp. 1–5.

[12] C. Sertatıl, M. A. Altınkaya, and K. Raoof, "A novel acoustic indoor localization system employing cdma," Digital Signal Processing, vol. 22, no. 3, 2012, pp. 506–517.

[13] J. Chen, J. Benesty, and Y. A. Huang, "Time delay estimation in room acoustic environments: an overview," EURASIP Journal on Advances in Signal Processing, vol. 2006, no. 1, 2006, pp. 1–19.

[14] I. Rishabh, D. Kimber, and J. Adcock, "Indoor localization using controlled ambient sounds," in Proc. of IPIN, 2012, pp. 1–10.

[15] T. Akiyama, M. Nakamura, M. Sugimoto, and H. Hashizume, "Smart phone localization method using dual-carrier acoustic waves," in Proc. of IPIN, 2013, pp. 1–9.

[16] M. Nakamura, T. Akiyama, M. Sugimoto, and H. Hashizume, "3d fdm-pam: Rapid and precise indoor 3d localization using acoustic signal for smartphone," in Proc. of UbiComp, 2014, pp. 123–126.

[17] H. Hashizume, A. Kaneko, Y. Sugano, K. Yatani, and M. Sugimoto, "Fast and Accurate Positioning Technique Using Ultrasonic Phase Accordance Method," in Proc. of IEEE TENCON, 2005, pp. 1–6.

[18] M. Nakamura, T. Akiyama, H. Hashizume, and M. Sugimoto, "A spot-controllable data transfer technique using cots speakers," in Proc. of IPIN, 2016, pp. 1–8.